Mathematical and Computer Modelling of Dynamical Systems
Vol. 00, No. 00, January 2006, 1–11

Multi-Parameter Polynomial Order Reduction of Linear Finite Element Models

Ortwin Farle*, Volker Hill, Pär Ingelström and Romanus Dyczij-Edlinger

Lehrstuhl für Theoretische Elektrotechnik, Saarland University,
P.O. Box 151150, D-66041 Saarbrücken, Germany
Phone: +49 (0)681 302-3194, Fax: +49 (0)681 302-3157

In this paper we present a numerically stable method for the model order reduction of finite element (FE) approximations to passive microwave structures parameterized by polynomials in several variables. The proposed method is a projection-based approach using Krylov subspaces and extends the works of [1] and [2]. First, we present the multivariate Krylov space of higher order associated with a parameter-dependent right-hand-side vector and derive a general recursion for generating its basis. Next, we propose an advanced algorithm to compute such basis in a numerically stable way. Finally, we apply the Krylov basis to construct a reduced order model of the moment-matching type. The resulting single-point method requires one matrix factorization only. Numerical examples demonstrate the efficiency and reliability of our approach.

Keywords: Multi-parameter system, model order reduction, moment-matching, robust numerical algorithms

AMS Subject Classification: 65F30; 65N30; 93A15; 93B25; 93B40

1. Introduction

The need for broadband frequency response simulations of electrical circuits with $n > 100000$ degrees of freedom led to the development of Krylov subspace based model order reduction (MOR) approaches. These methods finally found their way into the computational electromagnetics community, where they were mainly used in the context of finite element (FE) analysis.

The first widely used MOR method was the *asymptotic waveform evaluation* (AWE) [3]. In this approach, the transfer function of the system is first expanded in a Taylor series about a given expansion point, and, in a second step, a Padé-approximation matching the Taylor coefficients, the so called moments, is constructed. The resulting reduced order models (ROM) are of very low dimension, $q \ll n$, and can be evaluated very efficiently. However, the direct moment computation in AWE leads to numerical instabilities that limit the bandwidth attainable. To overcome this deficiency, multi-point methods like *complex frequency hopping* (CFH) [4] and multi-point Padé-approximation [5] were developed. One disadvantage of multi-point methods is the need for a separate matrix factorization at every expansion point. As a cheaper alternative, numerically robust one-point methods, such as the *Padé via Lanczos*-Algorithmus (PVL) [6, 7], were proposed. These methods perform moment-matching only implicitly. The *multi-point rational interpolation* method [8] achieves a further increase in numerical stability by combining the latter ideas with multi-point methods to construct rational Krylov sequences [9].

All the above methods assume linear parameter dependence. It is always possible to linearize polynomially parameterized systems, but this comes along with increased vector lengths [10], which results in an additional memory consumption. Conversely, the number of matching moments can be doubled by back-converting a first order system to higher order [11]. An attractive alternative to linearization, avoiding the vector length increase, is the use of Krylov spaces of higher order [12]. Modern methods using this approach are presented in [2] and [13].

*Corresponding author. Email: o.farle@lte.uni-saarland.de

Mathematical and Computer Modelling of Dynamical Systems
ISSN: 1387-3954 print/ISSN 1744-5051 online
http://www.tandf.co.uk/journals
DOI: 10.1080/1387395YYxxxxxxxx

In recent times, MOR has been extended to multi-parameter systems [1, 14]. Additional parameters are, e.g., wire spacings [15] or incident angles [16]. While most of these methods are restricted to linear parameterization, [1] presents an extension to polynomials in two parameters.

To our knowledge, most methods available for the multivariate case use direct moment computation and therefore suffer from the same numerical instabilities as the AWE. Only in [17] a first approach to increase the numerical stability is presented. The algorithm presented therein is restricted to linear parameterization. To overcome these difficulties, we present an advanced algorithm for computing well-conditioned bases for the Krylov spaces of systems parameterized by polynomials in several variables.

2. Systems Parameterized by Multivariate Polynomials

For clarity, we restrict ourselves to a system parameterized by a quadratic polynomial in two parameters s_1 and s_2,

$$\begin{aligned}\left(\mathbf{A}_{00}+s_1\mathbf{A}_{10}+s_2\mathbf{A}_{01}+s_1^2\mathbf{A}_{20}+s_1s_2\mathbf{A}_{11}+s_2^2\mathbf{A}_{02}\right)\mathbf{x}&\\ =\left(\mathbf{b}_{00}+s_1\mathbf{b}_{10}+s_2\mathbf{b}_{01}+s_1^2\mathbf{b}_{20}+s_1s_2\mathbf{b}_{11}+s_2^2\mathbf{b}_{02}\right)u,&\quad(1a)\\ y=\mathbf{c}^*\mathbf{x},&\quad(1b)\end{aligned}$$

where $\mathbf{A}_{kl}\in\mathbb{C}^{n\times n}$ for $k,l\in\{0,1,2\}$ and $\mathbf{x},\mathbf{b}_{kl},\mathbf{c}\in\mathbb{C}^n$. Here, superscript "*" denotes the transposed complex conjugate. The matrix $\mathbf{A}_{00}$, denoting the FE system matrix at the expansion point $(s_1=0,s_2=0)$, is assumed to be non-singular. From (1), we obtain a parameter-dependent transfer function $H(s_1,s_2)$ of the form

$$\begin{aligned}H(s_1,s_2)=\mathbf{c}^*\left(\mathbf{A}_{00}+s_1\mathbf{A}_{10}+s_2\mathbf{A}_{01}+s_1^2\mathbf{A}_{20}+s_1s_2\mathbf{A}_{11}+s_2^2\mathbf{A}_{02}\right)^{-1}&\\ \times\left(\mathbf{b}_0+s_1\mathbf{b}_{10}+s_2\mathbf{b}_{01}+s_1^2\mathbf{b}_{20}+s_1s_2\mathbf{b}_{11}+s_2^2\mathbf{b}_{02}\right).&\quad(2)\end{aligned}$$

3. Projection-Based Model Order Reduction

Similarly to the one-parameter case [8], MOR is achieved by projecting the system (1) on a lower dimensional subspace of dimension $m\ll n$. Let $\mathbf{v}_1,\mathbf{v}_2,\ldots,\mathbf{v}_m\in\mathbb{C}^n$ be mutually orthonormal global shape functions, and the matrix $\mathbf{V}$ be defined as

$$\mathbf{V}=[\mathbf{v}_1\mathbf{v}_2\ldots\mathbf{v}_m].\quad(3)$$

Then the restriction to $\mathrm{colsp}\{\mathbf{V}\}$ of the solution $\mathbf{x}$ of (1a) is expressed in terms of a reduced order solution $\hat{\mathbf{x}}\in\mathbb{C}^m$ as

$$\mathbf{x}=\mathbf{V}\hat{\mathbf{x}}.\quad(4)$$

Next, a Petrov-projection with the orthonormal test matrix $\mathbf{W}\in\mathbb{C}^{n\times m}$ gives the reduced system

$$\begin{aligned}\mathbf{W}^*\left(\mathbf{A}_{00}+s_1\mathbf{A}_{10}+s_2\mathbf{A}_{01}+s_1^2\mathbf{A}_{20}+s_1s_2\mathbf{A}_{11}+s_2^2\mathbf{A}_{02}\right)\mathbf{V}\hat{\mathbf{x}}&\\ =\mathbf{W}^*\left(\mathbf{b}_{00}+s_1\mathbf{b}_{10}+s_2\mathbf{b}_{01}+s_1^2\mathbf{b}_{20}+s_1s_2\mathbf{b}_{11}+s_2^2\mathbf{b}_{02}\right)u,&\quad(5a)\\ y=\mathbf{c}^*\mathbf{V}\hat{\mathbf{x}}.&\quad(5b)\end{aligned}$$

With the abbreviations

$$\hat{\mathbf{A}}_{kl}:=\mathbf{W}^*\mathbf{A}_{kl}\mathbf{V},\quad(6a)$$

$$\hat{\mathbf{b}}_{kl} := \mathbf{W}^* \mathbf{b}_{kl}, \tag{6b}$$

$$\hat{\mathbf{c}} := \mathbf{V}^* \mathbf{c}, \tag{6c}$$

we obtain the reduced order system

$$\begin{aligned} &\left(\hat{\mathbf{A}}_{00} + s_1\hat{\mathbf{A}}_{10} + s_2\hat{\mathbf{A}}_{01} + s_1^2\hat{\mathbf{A}}_{20} + s_1s_2\hat{\mathbf{A}}_{11} + s_2^2\hat{\mathbf{A}}_{02}\right)\hat{\mathbf{x}} \\ &= \left(\hat{\mathbf{b}}_{00} + s_1\hat{\mathbf{b}}_{10} + s_2\hat{\mathbf{b}}_{01} + s_1^2\hat{\mathbf{b}}_{20} + s_1s_2\hat{\mathbf{b}}_{11} + s_2^2\hat{\mathbf{b}}_{02}\right)u, \end{aligned} \tag{7a}$$

$$y = \hat{\mathbf{c}}^*\hat{\mathbf{x}} \tag{7b}$$

and its transfer function

$$\begin{aligned} \hat{H}(s_1,s_2) = \mathbf{c}^* &\left(\hat{\mathbf{A}}_{00} + s_1\hat{\mathbf{A}}_{10} + s_2\hat{\mathbf{A}}_{01} + s_1^2\hat{\mathbf{A}}_{20} + s_1s_2\hat{\mathbf{A}}_{11} + s_2^2\hat{\mathbf{A}}_{02}\right)^{-1} \\ &\times \left(\hat{\mathbf{b}}_0 + s_1\hat{\mathbf{b}}_{10} + s_2\hat{\mathbf{b}}_{01} + s_1^2\hat{\mathbf{b}}_{20} + s_1s_2\hat{\mathbf{b}}_{11} + s_2^2\hat{\mathbf{b}}_{02}\right). \end{aligned} \tag{8}$$

Since (7) is of very low dimension, it can be evaluated very efficiently at any point (s_1, s_2) in parameter space. From the reduced order solution $\hat{\mathbf{x}}$, the FE-solution can be reconstructed via (4). The quality of the ROM is determined by the dimension m and, most importantly, the choice of trial space colsp$\{\mathbf{V}\}$ and test space colsp$\{\mathbf{W}\}$, respectively.

4. Choice of Trial Space

We now show how to choose colsp$\{\mathbf{V}\}$ to achieve moment-matching between $\hat{H}(s_1, s_2)$ and $H(s_1, s_2)$. For this purpose, we set without loss of generality $u = 1$ and expand the solution vector $\mathbf{x}$ of (1a) in a Taylor series. We get

$$\begin{aligned} &\left(\mathbf{A}_{00} + s_1\mathbf{A}_{10} + s_2\mathbf{A}_{01} + s_1^2\mathbf{A}_{20} + s_1s_2\mathbf{A}_{11} + s_2^2\mathbf{A}_{02}\right)\left(\sum_{e=0}^{\infty}\sum_{i=0}^{e} s_1^i s_2^{e-i}\mathbf{x}_{i,e-i}\right) \\ &= \mathbf{b}_{00} + s_1\mathbf{b}_{10} + s_2\mathbf{b}_{01} + s_1^2\mathbf{b}_{20} + s_1s_2\mathbf{b}_{11} + s_2^2\mathbf{b}_{02}. \end{aligned} \tag{9}$$

By comparison of coefficients, we have

$$\mathbf{x}_{00} = \mathbf{A}_{00}^{-1}\mathbf{b}_{00} \tag{10a}$$

$$\mathbf{x}_{10} = \mathbf{A}_{00}^{-1}\left(\mathbf{b}_{10} - \mathbf{A}_{10}\mathbf{x}_{00}\right) \tag{10b}$$

$$\mathbf{x}_{01} = \mathbf{A}_{00}^{-1}\left(\mathbf{b}_{01} - \mathbf{A}_{01}\mathbf{x}_{00}\right) \tag{10c}$$

$$\mathbf{x}_{20} = \mathbf{A}_{00}^{-1}\left(\mathbf{b}_{20} - \mathbf{A}_{10}\mathbf{x}_{10} - \mathbf{A}_{20}\mathbf{x}_{00}\right) \tag{10d}$$

$$\mathbf{x}_{11} = \mathbf{A}_{00}^{-1}\left(\mathbf{b}_{11} - \mathbf{A}_{10}\mathbf{x}_{01} - \mathbf{A}_{01}\mathbf{x}_{10} - \mathbf{A}_{11}\mathbf{x}_{00}\right) \tag{10e}$$

$$\mathbf{x}_{02} = \mathbf{A}_{00}^{-1}\left(\mathbf{b}_{02} - \mathbf{A}_{01}\mathbf{x}_{01} - \mathbf{A}_{02}\mathbf{x}_{00}\right) \tag{10f}$$

$$\mathbf{x}_{30} = \mathbf{A}_{00}^{-1}\left(-\mathbf{A}_{10}\mathbf{x}_{20} - \mathbf{A}_{20}\mathbf{x}_{10}\right) \tag{10g}$$

$$\vdots$$

$$\mathbf{x}_{ij} = \mathbf{A}_{00}^{-1}\left(-\mathbf{A}_{10}\mathbf{x}_{i-1,j} - \mathbf{A}_{01}\mathbf{x}_{i,j-1} - \mathbf{A}_{20}\mathbf{x}_{i-2,j} - \mathbf{A}_{11}\mathbf{x}_{i-1,j-1} - \mathbf{A}_{02}\mathbf{x}_{i,j-2}\right). \tag{10h}$$

The recursion (10) defines a parameter-independent *multivariate Krylov space $\mathcal{K}$ of order two*. More specifically, we denote by $\mathcal{K}_q\left(\mathbf{A}_{00}^{-1}\mathbf{A}_{kl}, \mathbf{A}_{00}^{-1}\mathbf{b}_{kl}\right)$, with $k, l \in \{0, 1, 2\}$ the subspace of all moments $\mathbf{x}_{ij}$ with

$i + j \leq q$,

$$\mathcal{K}_q\left(\mathbf{A}_{00}^{-1}\mathbf{A}_{kl}, \mathbf{A}_{00}^{-1}\mathbf{b}_{kl}\right) = \text{span}\{\mathbf{x}_{ij} | i + j \leq q\}. \tag{11}$$

The recursion (10) implies that, when the trial matrix $\mathbf{V}$ is chosen such that

$$\text{colsp}\mathbf{V} = \mathcal{K}_q\left(\mathbf{A}_{00}^{-1}\mathbf{A}_{kl}, \mathbf{A}_{00}^{-1}\mathbf{b}_{kl}\right), \tag{12}$$

the leading q derivatives with respect to s_1 and s_2 of the ROM (12) will coincide with those of the original model at the expansion point.

$$\left.\frac{\partial^{i+j}\hat{H}}{\partial s_1^i \partial s_2^j}\right|_{s_1=s_2=0} = \left.\frac{\partial^{i+j}H}{\partial s_1^i \partial s_2^j}\right|_{s_1=s_2=0} \qquad \text{for } 0 \leq i + j \leq q. \tag{13}$$

The proof of (13) is by induction. Because of its great similarity to that for parameter-independent right-hand-sides [1], details are omitted.

4.1. *General case*

For a linear system of equations parameterized by a polynomial of degree M in N scalar parameters, we write

$$\left(\sum_{|\alpha|\leq M} \mathbf{s}^\alpha \mathbf{A}_\alpha\right)\mathbf{x} = \left(\sum_{|\alpha|\leq M} \mathbf{s}^\alpha \mathbf{b}_\alpha\right) u, \tag{14a}$$

$$y = \mathbf{c}^*\mathbf{x}, \tag{14b}$$

where $\alpha = (\alpha_1, \alpha_2, \ldots, \alpha_N)$ is a multi-index, and $\mathbf{s}^\alpha$ is defined as

$$\mathbf{s}^\alpha = s_1^{\alpha_1} s_2^{\alpha_2} \ldots s_N^{\alpha_N}. \tag{15}$$

With the multi-index $\beta = (\beta_1, \beta_2, \ldots, \beta_N)$, the moments $\mathbf{x}_\beta$ are found from (10) to be

$$\mathbf{x}_\beta = \mathbf{A}_{\alpha=0}^{-1}\left(\mathbf{b}_\beta - \sum_{|\alpha|=1}^{|\alpha|\leq M} \mathbf{A}_\alpha \mathbf{x}_{\beta-\alpha}\right), \tag{16}$$

where $\mathbf{x}_\beta = \mathbf{0}$ for $\beta_i < 0$. In analogy to (12), any projection matrix $\mathbf{V}$ with

$$\text{colsp}\{\mathbf{V}\} = \mathcal{K}_q\left(\mathbf{A}_\alpha, \mathbf{b}_\alpha\right) = \text{span}\left\{\bigcup_{|\beta|\leq q} \mathbf{A}_{\alpha=0}^{-1}\left(\mathbf{b}_\beta - \sum_{|\alpha|=1}^{|\alpha|\leq M} \mathbf{A}_\alpha \mathbf{x}_{\beta-\alpha}\right)\right\}. \tag{17}$$

generates a ROM that matches the first q moments of the transfer function of the original system.

5. Choice of Test Space

The order of matching derivatives can be increased to $2q + 1$ [14] by choosing $\mathbf{W}$ such that

$$\mathbf{W}^*\mathbf{V} = \mathbf{I}, \tag{18}$$

$$\mathrm{colsp}\{\mathbf{W}\} = \mathrm{span}\{\mathbf{y}_{ij}\}, \tag{19}$$

where

$$\mathbf{y}_{ij} = \mathbf{A}_{00}^{*-1}\left(\mathbf{c}_{ij} - \sum_{k,l}\mathbf{A}_{kl}^{*}\mathbf{y}_{i-k,j-l}\right) \qquad \text{with } i,j \geq 0 \text{ and } i+j \leq q. \tag{20}$$

Note that, in the prototype problem (1), we have $\mathbf{c}_{ij} = \mathbf{0}$ for $i, j \neq 0$ and $\mathbf{A}_{kl} = \mathbf{0}$ if $k, l \notin \{0, 1, 2\}$.

One disadvantage of oblique subspace projections is that important algebraic properties of the original matrices do not carry over the reduced order system. To preserve definiteness and Hermitian structure, we propose to always use Galerkin projections

$$\mathbf{W} = \mathbf{V}. \tag{21}$$

As a result, the ROM inherits essential system properties, like passivity, from the original model [18, 19]. We also mention that there are important applications, such as the FE-simulation of lossless, reciprocal microwave systems, which lead to real symmetric matrices and $\mathbf{c} = \mathbf{b}$. In these cases, the Galerkin projection (21) matches $2q + 1$ derivatives, too.

6. Computation of Projection Basis

Present multi-parameter methods build the matrix $\mathbf{V}$ by explicit computation of the Krylov basis via (10) and subsequent orthogonalization [1, 14–16]. With increasing order q, this approach suffers from numerical cancellation. As a rationale, consider the moments $\mathbf{x}_{i0}$, $i = 0, \ldots, q$. They are identical to the one-parameter case with $s = s_1$, and it is well known that their direct computation is ill-conditioned [2]. One-parameter methods overcome this difficulty by using the Arnoldi or Lanczos algorithm [2, 6, 7, 20] to compute a stable basis. In the following, we present a similar method for the multivariate case.

6.1. *Proposed Algorithm*

Our goal is to construct an orthonormal basis $\mathbf{V}$ for the Krylov space $\mathcal{K}_q\left(\mathbf{A}_{00}^{-1}\mathbf{A}_{kl},\ \mathbf{A}_{00}^{-1}\mathbf{b}_{kl}\right)$ and replace the sequence (10) by a numerically more robust recursion.

Our starting point is the extension of the p-column basis $\mathbf{V}_p = [\mathbf{v}_1 \ldots \mathbf{v}_p]$ by the moment vector $\mathbf{x}_{ij}$ of degree $s = i + j$. Since $\mathbf{V}_p$ is built from the precursors of $\mathbf{x}_{ij}$, (11) and (12) imply that all $\mathbf{x}_{cd}$ with degree $c + d < s$ lie in $\mathrm{colsp}\{\mathbf{V}_p\}$. Hence there exists a coordinate vector $\mathbf{h}_{cd}$ such that

$$\mathbf{x}_{cd} = \mathbf{V}_p\mathbf{h}_{cd}. \tag{22}$$

Specifically, the start vector of recursion (10) is associated with vectors $\mathbf{v}_1$ and $\mathbf{h}_{00}$ of the form

$$\mathbf{v}_1 = \mathbf{A}_{00}^{-1}\mathbf{b}_{00}/\|\mathbf{A}_{00}^{-1}\mathbf{b}_{00}\|, \tag{23}$$

$$\mathbf{h}_{00} = \|\mathbf{A}_{00}^{-1}\mathbf{b}_{00}\|\mathbf{e}_1. \tag{24}$$

By expanding all precursors of $\mathbf{x}_{ij}$ in terms of (22), recursion (10) yields the representation

$$\mathbf{x}_{ij} = \mathbf{A}_{00}^{-1}\mathbf{b}_{ij} - \sum_{k,l}\mathbf{A}_{00}^{-1}\mathbf{A}_{kl}\mathbf{V}_p\mathbf{h}_{i-k,j-l} \qquad \text{with } k,l \in \{0,1,2\}, \quad k+l > 0. \tag{25}$$

In the following, we decompose (25) into components in $\mathrm{colsp}\{\mathbf{V}_p\}$ and an orthogonal complement to be employed as the basis vector $\mathbf{v}_{p+1}$. With the help of the complementary orthonormal projectors $\mathbf{V}_p\mathbf{V}_p^*$ and

$\mathbf{I} - \mathbf{V}_p\mathbf{V}_p^*$, we have

$$\mathbf{A}_{00}^{-1}\mathbf{b}_{ij} = \mathbf{V}_p\mathbf{V}_p^*\mathbf{A}_{00}^{-1}\mathbf{b}_{ij} + \left(\mathbf{I} - \mathbf{V}_p\mathbf{V}_p^*\right)\mathbf{A}_{00}^{-1}\mathbf{b}_{ij}. \tag{26}$$

Similarly, we split in (25) the matrices $\mathbf{A}_{00}^{-1}\mathbf{A}_{kl}\mathbf{V}_p$ into components in $\mathrm{colsp}\{\mathbf{V}_p\}$ with coordinates $\mathbf{C}_{kl}^p$ and orthogonal remainders $\mathbf{R}_{kl}^p$,

$$\mathbf{A}_{00}^{-1}\mathbf{A}_{kl}\mathbf{V}_p = \mathbf{V}_p\mathbf{C}_{kl}^p + \mathbf{R}_{kl}^p, \tag{27}$$

$$\mathbf{V}_p^*\mathbf{R}_{kl}^p = \mathbf{0}. \tag{28}$$

The matrices $\mathbf{C}_{kl}^p$ and $\mathbf{R}_{kl}^p$ are readily obtained: after pre-multiplying (27) by $\mathbf{V}_p^*$, the orthogonality relation (28) yields

$$\mathbf{C}_{kl}^p = \mathbf{V}_p^*\mathbf{A}_{00}^{-1}\mathbf{A}_{kl}\mathbf{V}_p, \tag{29}$$

and insertion of $\mathbf{C}_{kl}^p$ into (27) gives $\mathbf{R}_{kl}^p$. By plugging (26) and (27) into (25), we obtain the representation

$$\mathbf{x}_{ij} = \mathbf{V}_p\mathbf{V}_p^*\mathbf{A}_{00}^{-1}\mathbf{b}_{ij} - \mathbf{V}_p\sum_{k,l}\mathbf{C}_{kl}^p\mathbf{h}_{i-k,j-l} + \left(\mathbf{I} - \mathbf{V}_p\mathbf{V}_p^*\right)\mathbf{A}_{00}^{-1}\mathbf{b}_{ij} - \sum_{k,l}\mathbf{R}_{kl}^p\mathbf{h}_{i-k,j-l}. \tag{30}$$

Evidently, the first two expressions are in $\mathrm{colsp}\{\mathbf{V}_p\}$, whereas the remaining ones are orthogonal to $\mathbf{V}_p$. With the abbreviations

$$\mathbf{h}_{\|} = -\sum_{k,l}\mathbf{C}_{kl}^p\mathbf{h}_{i-k,j-l} + \mathbf{V}_p^*\mathbf{A}_{00}^{-1}\mathbf{b}_{ij}, \tag{31}$$

$$\mathbf{x}_{\perp} = -\sum_{k,l}\mathbf{R}_{kl}^p\mathbf{h}_{i-k,j-l} + \left(\mathbf{I} - \mathbf{V}\mathbf{V}^*\right)\mathbf{A}_{00}^{-1}\mathbf{b}_{ij}, \tag{32}$$

the moment $\mathbf{x}_{ij}$ takes the form

$$\mathbf{x}_{ij} = \mathbf{V}_p\mathbf{h}_{\|} + \mathbf{x}_{\perp}. \tag{33}$$

Since $\mathbf{x}_{\perp}$ is orthogonal to $\mathbf{V}_p$, the new basis vector $\mathbf{v}_{p+1}$ is determined by

$$\mathbf{v}_{p+1} = \mathbf{x}_{\perp}/\|\mathbf{x}_{\perp}\|. \tag{34}$$

Finally, by plugging (33) and (34) into the expansion formula (22),

$$\mathbf{x}_{ij} = [\mathbf{V}_p, \mathbf{v}_{p+1}]\begin{bmatrix}\mathbf{h}_{\|}\\ \|\mathbf{x}_{\perp}\|\end{bmatrix}, \tag{35}$$

the new coordinate vector $\mathbf{h}_{ij}$ is seen to be

$$\mathbf{h}_{ij} = \begin{bmatrix}\mathbf{h}_{\|}\\ \|\mathbf{x}_{\perp}\|\end{bmatrix}. \tag{36}$$

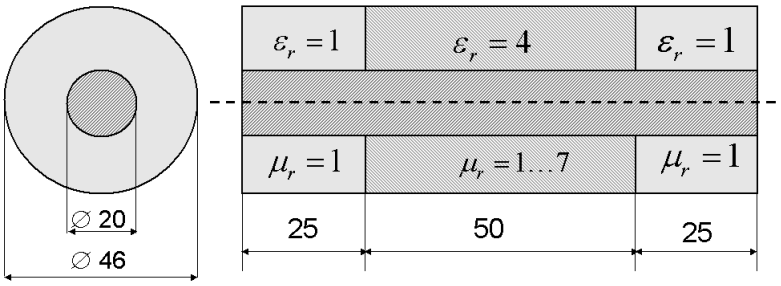

Figure 1. Coaxial probe. Geometry and material data. All dimensions are in mm.

Thus, the algorithm we propose reads as follows:

Given: $\mathbf{A}_{cd}, \mathbf{b}_{cd}$.

Init: $\mathbf{v}_1 = \mathbf{A}_{00}^{-1}\mathbf{b}_{00}/\|\mathbf{A}_{00}^{-1}\mathbf{b}_{00}\|, \mathbf{h}_{00} = \|\mathbf{A}_{00}^{-1}\mathbf{b}_{00}\|\mathbf{e}_1, p = 1.$

Iter: FOR $o = 1 : q$, FOR $j = 0 : o, i = o - p$

Compute $\mathbf{C}_{kl}^p$ from (29)

Compute $\mathbf{R}_{kl}^p$ from (27)

Compute $\mathbf{h}_{\|}$ from (31) and $\mathbf{x}_{\perp}$ from (32)

Set $\mathbf{v}_{p+1} = \mathbf{x}_{\perp}/\|\mathbf{x}_{\perp}\|$ and $\mathbf{h}_{ij} = \begin{bmatrix} \mathbf{h}_{\|} \\ \|\mathbf{f}_{\perp}\| \end{bmatrix}$

$p \leftarrow p + 1$

END j, END o.

Note that the matrices $\mathbf{C}_{cd}^p$ need not be constructed from scratch at every iteration step. Just their pth rows and columns have to be computed. Moreover, the matrices $\mathbf{R}_{cd}^p$ can be updated very efficiently by orthogonalizing their rows against $\mathbf{v}_p$.

7. Numerical Examples

7.1. *Multivariate Linearly Parameterized System*

Fig. 1 shows a coaxial line with toroid-shaped inset. For this simple structure, analytical solutions are easily obtained. The system response is given by the reflection coefficient S_{11} as a function of frequency f and inset permeability μ_r, where the parameter domain is defined by $f = 1 \ldots 4.5\,\text{GHz}$ and $\mu_r = 1 \ldots 7$. We purposely choose the expansion point at (f = 3 GHz, $\mu_r = 4$), such that there is no reflection at all and construct a ROM of order $q = 10$. Since the structure is a two-port device, the resulting ROM is of dimension $2 \cdot (q + 1) \cdot (q + 2)/2 = 132$. Fig. 2 depicts the response surface for $|S_{11}|$, sampled by $201 \times 201 = 40401$ points. The CPU-time for computing all 40401 ROM solutions on a 2.2 GHz Pentium IV processor is less than 200 s, whereas the same number of full FE simulations would take 258 hours. Fig. 3 gives the magnitude of the error in reflection coefficient |Error S_{11}|,

$$|\text{Error } S_{11}| = |S_{11}^{ROM} - S_{11}^{ref}|, \tag{37}$$

where the analytical solution is taken as the reference S_{11}^{ref}. It can be seen that the error is typically in the order of 10^{-4} and increases to 10^{-2} in the vicinity of ($f = 4.5$ GHz, $\mu_r = 7$), where the resolution of the FE mesh is worst. For comparison with previous methods, we have constructed a model of same dimension by direct implementation of (10) followed by an orthogonalization step after the building process. The error

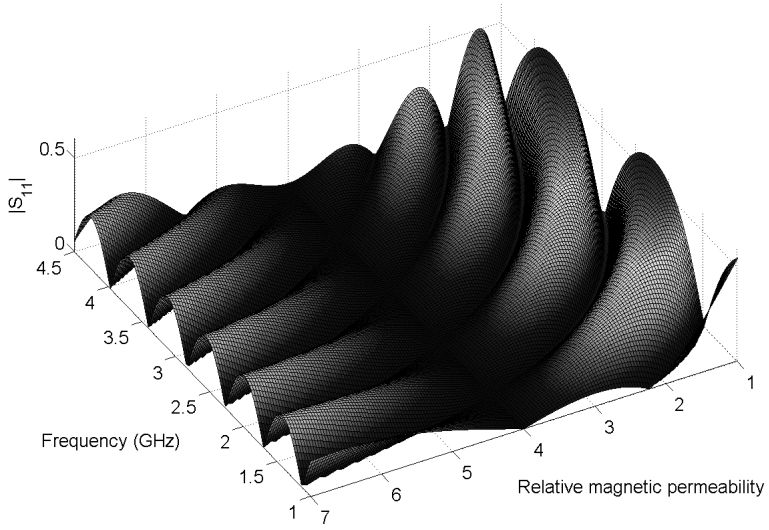

Figure 2. Coaxial probe. Magnitude of reflection coefficient as a function of frequency and relative permeability, as computed by the proposed algorithm.

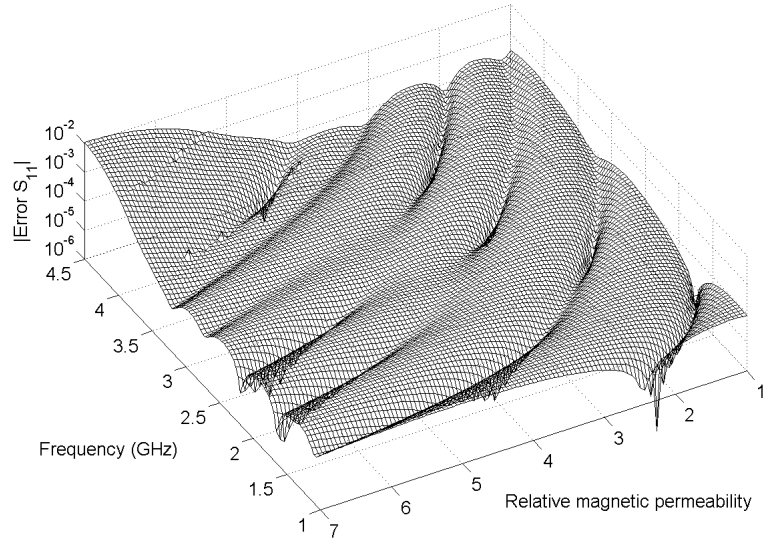

Figure 3. Coaxial probe. Magnitude of error in reflection coefficient (37) as a function of frequency and relative permeability.

plot of Fig. 4 shows that these results are far off.

7.2. *Multivariate Polynomially Parameterized System*

We now consider the patch antenna of Fig. 5. The system response is the reflection coefficient S_{11} as a function of frequency $f = 3 \ldots 8\,\mathrm{GHz}$ and the relative permittivity values of the two dielectrics $\varepsilon_{r1} = 1 \ldots 5$, $\varepsilon_{r2} = 1 \ldots 3$. Motivated by the authors' previous analysis of that specific design, the expansion point is chosen at ($f = 6$ GHz, $\varepsilon_{r1} = 4$, $\varepsilon_{r2} = 2$). A FE approach [22] using absorbing boundary conditions and transfinite elements [23] results in a linear system of equations of the form

$$\left(\mathbf{S} - \omega^2 \mathbf{T}\left(\varepsilon_1, \varepsilon_2\right) + \omega \mathbf{T}^{ABC} + j\omega\tilde{\mathbf{I}}\right)\mathbf{x} = \omega \mathbf{b} \tag{38}$$

with $n = 58247$ degrees of freedom. We introduce the parameters

$$\omega = \bar{\omega}\left(1 + s_1\right), \qquad \varepsilon_1 = \bar{\varepsilon}_1\left(1 + s_2\right), \qquad \varepsilon_2 = \bar{\varepsilon}_2\left(1 + s_3\right), \tag{39}$$

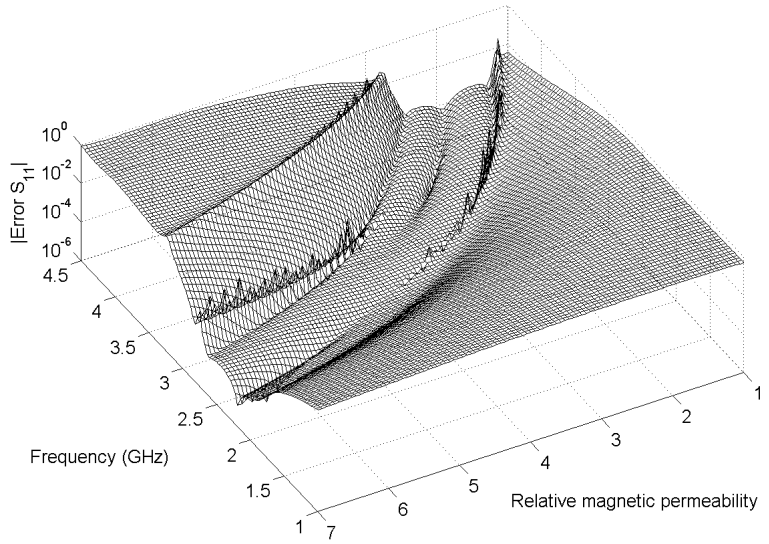

Figure 4. Coaxial probe. Magnitude of error in reflection coefficient (37) as a function of frequency and relative permeability computed by direct implementation of definition (10) and post-orthogonalization.

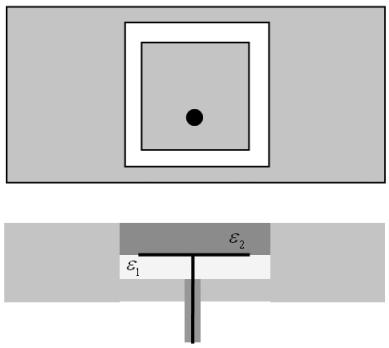

Figure 5. Patch antenna. Schematic of the geometry, featuring two different dielectrics. Dimensions are given in [21].

where $\bar{\omega}$, $\bar{\varepsilon}_1$, and $\bar{\varepsilon}_2$ denote nominal values at the expansion point. By plugging (39) into (38), we obtain the polynomially parameterized system of equations

$$\begin{aligned}&\Big(\mathbf{S} - \bar{\omega}^2\mathbf{T} + \bar{\omega}\mathbf{T}^{ABC} + j\bar{\omega}\tilde{\mathbf{I}} - s_1\left(2\bar{\omega}^2\mathbf{T} - j\bar{\omega}\tilde{\mathbf{I}} - \bar{\omega}\mathbf{T}^{ABC}\right)\\ &-s_2\bar{\omega}^2\mathbf{T}^{\varepsilon_1} - s_3\bar{\omega}^2\mathbf{T}^{\varepsilon_2} - s_1^2\bar{\omega}^2\mathbf{T} - s_1s_2 2\bar{\omega}^2\mathbf{T}^{\varepsilon_1} - s_1s_3 2\bar{\omega}^2\mathbf{T}^{\varepsilon_2}\\ &-s_1^2s_2\bar{\omega}^2\mathbf{T}^{\varepsilon_1} - s_1^2s_3\bar{\omega}^2\mathbf{T}^{\varepsilon_2}\Big)\,\mathbf{x} = \omega\mathbf{b}.\end{aligned} \tag{40}$$

Note that, by $s_1^2s_2\mathbf{T}^{\varepsilon_1}$ and $s_1^2s_3\mathbf{T}^{\varepsilon_2}$, terms of third degree are present. The order of the reduced model is chosen to be $q = 8$, and the resulting model dimension is 165. Fig. 6 shows a two-dimensional cut through the three-dimensional response hyper-surface. To assess the accuracy of the ROM, we need to compute reference values S_{11}^{ref} by full FE runs, because analytic solutions are not available. Since such calculations are very time-consuming, we are unable to present error data for the two-dimensional cut of Fig. 6. Instead, we just consider a line placed at one outer edge of the parameter domain ($\varepsilon_{r1} = 1, \varepsilon_{r2} = 3$), sampled by 51 equidistant points. The corresponding solutions and errors (37) are given in Fig. 7 and Fig. 8, respectively. Again, accuracy is very satisfactory.

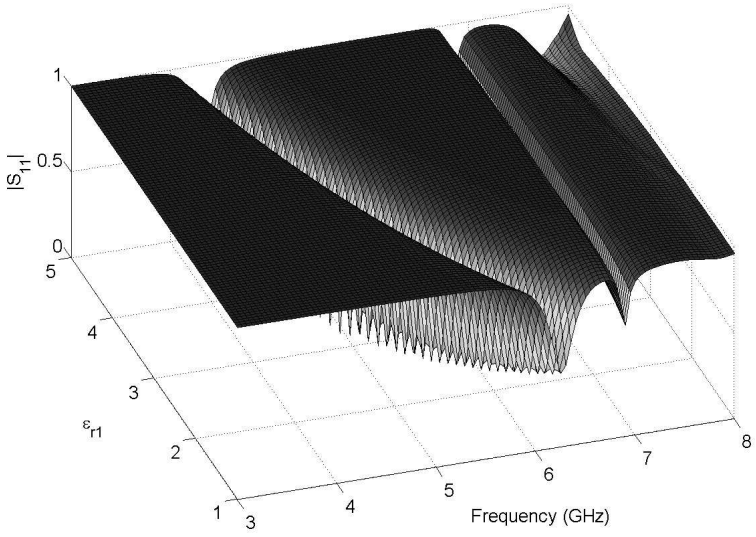

Figure 6. Patch Antenna. Magnitude of reflection coefficient at $\varepsilon_{r2} = 3$ as a function of frequency and relative permittivity ε_{r1}.

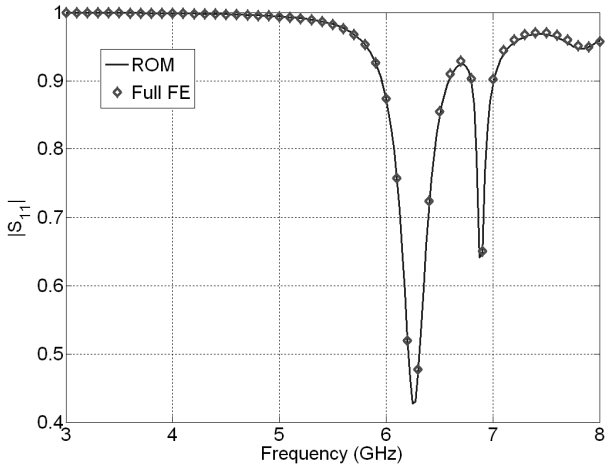

Figure 7. Patch Antenna. Comparison of ROM with full FE simulations for $\varepsilon_{r1} = 1$ and $\varepsilon_{r2} = 3$.

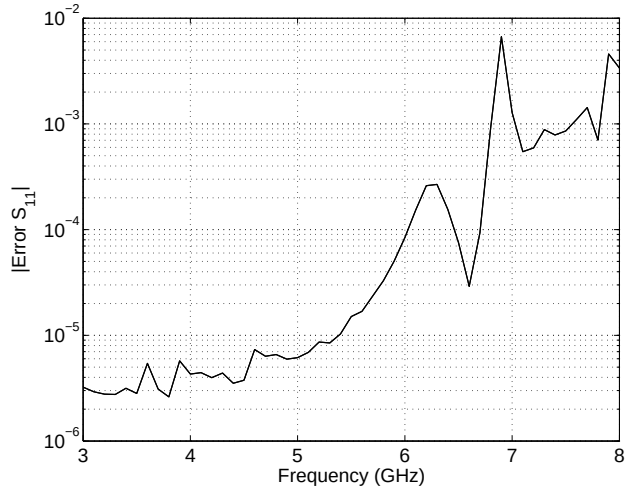

Figure 8. Patch Antenna. Magnitude of error in reflection coefficient (37) as a function of frequency. Parameters: $\varepsilon_{r1} = 1$, $\varepsilon_{r2} = 3$.

8. Summary and Outlook

We have presented a general recursion for the Krylov space of polynomially parameterized systems of linear equations with parameter-dependent right-hand-sides. In addition, we have proposed an algorithm for computing a well-conditioned basis and a related single-point method for the order reduction of multi-parameter systems. Numerical examples validate the reliability of the suggested approach.

At present, the order of the ROM is set by the user directly. In the future, we intend to develop an error estimator that stops the MOR process automatically as soon as a pre-defined level of accuracy is obtained. Since the model dimension grows very rapidly when the number of parameters gets large, purging strategies that reduce the number of basis vectors without sacrificing accuracy are to be developed. Another goal of future work is to build an even more powerful tool for multivariate MOR by employing the single-point algorithm presented in this paper as a building block within a multi-point framework.

Acknowledgement

V. Hill was supported by a Grant from Ansoft Corporation. P. Ingelström was supported by a fellowship from the Alexander von Humboldt-Foundation.

References

[1] Gunupudi, P., Khazaka, R. and Nakhla, M., 2002, Analysis of transmission line circuits using multidimensional model reduction techniques, IEEE Trans. Adv. Packaging, vol. 25, no. 2, pp. 174-180.
[2] Slone, R.D., Lee, R. and Lee, J.-F., 2003, Broadband model order reduction of polynomial matrix equations using single-point well-conditioned asymptotic waveform evaluation: derivations and theory, Int. J. Numer. Meth. Engng., 58, pp. 2325-2342.
[3] Pillage, L.T. and Rohrer, R.A., 1990, Asymptotic waveform evaluation for timing analysis, IEEE Trans. Comp.-Aided Design Integrated Circuits, vol. 12, pp. 352-366.
[4] Chiprout, E. and Nakhla, M., 1993, Transient waveform estimation of high-speed MCM networks using complex frequency hopping, Proc. Multi-Chip Module Conference (MCMC), pp. 134-139.
[5] Celik, M., Ocali, O., Tan, M.A. and Atalar A., 1995, Pole-zero computation in microwave circuits using multi-point Padé approximation, IEEE Trans. Circuits Syst. I, 42, pp. 6-13.
[6] Feldmann, P. and Freund, R.W., 1995, Efficient linear circuit analysis by Padé approximation via the Lanczos process, IEEE Trans. Comp.-Aided Design Integrated Circuits, vol. 14, pp. 639-649.
[7] Gallivan, K., Grimme, E. and Van Dooren, P., 1994, Asymptotic waveform evaluation via a Lanczos method", Appl. Math. Lett., 7(5), pp. 75-80.
[8] Grimme, E., 1997, Krylov projection methods for model reduction, Ph.D. dissertation, Coordinated-Science Laboratory, Univ. of Illinois at Urbana-Champaign, Urbana-Champaign, IL.
[9] Ruhe, A., 1984, Rational Krylov sequence methods for eigenvalue computation", Lin. Alg. Appl., 58, pp. 391-405.
[10] Slone, R.D. and Lee, R., 2000, Applying Padé via Lanczos to the finite element method for electromagnetic radiation problems, Radio Science, vol. 35, no. 2, pp. 331-340.
[11] Salimbahrami, B. and Lohmann, B., 2006, Order Reduction of Large Scale Second Order Systems using Krylov Subspace Methods, Linear Algebra and its Application, vol. 415, no. 2-3, pp. 385-405. available online at www.sciencedirect.com.
[12] Su, T.J. and Craig Jr., R.R., 1989, Model reduction and control of flexible structures using Krylov vectors, J. Guidance 14, pp. 260-267.
[13] Bai, Z. and Su, Y., 2005, Dimension reduction of second-order dynamical systems via a second-order Arnoldi method, SIAM J. Sci. Comput., vol. 26, no. 5, pp. 1692-1709.
[14] Weile, D.S., Michielssen, E., Grimme, E. and Gallivan, K., 1999, A method for generating rational interpolant reduced order models of two-parameter linear systems, Applied Mathematics Letters, vol. 12, pp. 93-102.
[15] Daniel, L., Ong, C.S., Chay, L.S., Lee, K.H. and White, J., 2004, A multiparameter moment-matching model-reduction approach for generating geometrically parameterized interconnect performance models, IEEE Trans. Comp.-Aided Design Integrated Circuits, vol. 23, pp. 678-693.
[16] Weile, D.S. and Michielssen, E., 2001, Analysis of frequency selective surfaces using two-parameter generalized rational Krylov model-order reduction, IEEE Trans. Antennas Propagat., vol. 49, pp. 1539-1549.
[17] Codecasa L., 2005, A novel approach for generating boundary condition independent compact dynamic thermal networks of packages, IEEE Trans. Compononents Packaging, vol. 28, pp. 593-604.
[18] Odabasioglu, A., Celik, M. and Pileggi, L.T., 1998, PRIMA: Passive Reduced-Order Interconnect Macromodeling Algorithm, IEEE Trans. Comp.-Aided Design Integrated Circuits, vol. 17, no. 8, pp. 645-654.
[19] Freund, R.W., 2000, Passive Reduced-Order Modeling via Krylov Subspace Methods, Numerical Analysis Manuscript, (00-3-02), also available at URL http://cm.belllabs. com/cs/doc/00.
[20] Boley, D.L., 1994, Krylov space methods on state-space control models", Circuits Syst. Signal Processing, vol. 13, no. 6, pp. 733-758.
[21] González de Aza, M. A., Encinar, J.A., Zapata, J. and Lambae, M., 1998, Full-wave analysis of cavity-backed and probe-fed microstrip patch arrays by a hybrid mode-matching generalized scattering matrix and finite-element method, IEEE Trans. Antennas Propagat., vol. 46, pp. 234-242.
[22] Bossavit, A. and Mayergoyz, I., 1989, Edge-elements for scattering problems, IEEE Trans. Magn., vol. 25, no. 4, pp. 2816-2821.
[23] Cendes, Z.J. and Lee, J.-F., 1988, The Transfinite Element Method for Modeling MMIC Devices, IEEE Trans. Microwave Theory Tech., vol. 36, no. 12, pp. 1639-1649.